Plant Biotechnology Journal
Open Access

Plant Biotechnology Journal (2021) **19**, pp. 875–877 doi: 10.1111/pbi.13577

Brief Communication

Generation of novel self-incompatible *Brassica napus* by CRISPR/Cas9

Shengwei Dou[1], Tong Zhang[2], Jinxing Tu[1], Jinxiong Shen[1], Bin Yi[1], Jing Wen[3], Tingdong Fu[1], Cheng Dai[1,*] and Chaozhi Ma[1,*]

[1]*National Key Laboratory of Crop Genetic Improvement, Huazhong Agricultural University, Wuhan, China*
[2]*Key Laboratory of Horticultural Plant Biology (Ministry of Education), College of Horticulture and Forestry Sciences, Huazhong Agricultural University, Wuhan, China*
[3]*College of Plant Science and Technology, Huazhong Agricultural University, Wuhan, China*

Received 20 November 2020;
revised 17 February 2021;
accepted 27 February 2021.
**Correspondence* (Tel 86-027-87281507; emails cdai@mail.hzau.edu.cn (CD); yuanbeauty@mail.hzau.edu.cn (CM))
The authors responsible for the distribution of materials integral to the findings presented in this article in accordance with the policy described in the Instructions for Authors are: Dr. Cheng Dai (cdai@mail.hzau.edu.cn) and Dr. Chaozhi Ma (yuanbeauty@mail.hzau.edu.cn).

Keywords: *Brassica napus*, self-incompatibility, *BnS6-Smi2*, *BnSCR7*, DNA methylation, CRISPR, Cas9.

Self-incompatibility (SI) is a genetic mechanism that prevents inbreeding in hermaphrodite angiosperms via the rejection of self-pollen. SI lines facilitate the utilization of heterosis (Nettancourt, 2001). In cruciferous plants, SI is determined by the *S* locus, which harbors genes encoding the stigma papilla cell-specific S-receptor kinase (SRK) and the pollen surface-localized ligand of SRK, S-locus cysteine-rich protein/S-locus protein 11 (SCR/SP11) (Schopfer *et al.,* 1999; Suzuki *et al.,* 1999). *Brassica napus* is self-compatible (SC), even though it is generated from two SI species, *Brassica rapa* and *Brassica oleracea*. SI *B. napus* could be generated by introducing the *S* locus from *B. rapa* or/and *B. oleracea* into *B. napus* by interspecific hybridization or genetic transformation (Fu and Liu, 1975; Gao *et al.,* 2016). However, few *B. napus* SI lines are currently available due to the instability of offspring produced by interspecific hybridization, and silencing of the introduced *BrSCR* gene over several generations. One promising method for creating new *B. napus* SI lines is CRISPR/Cas9 genome editing (Chen *et al.,* 2019).

In *B. rapa*, the linear dominance hierarchy of class II S haplotype *SCR* alleles is controlled by *SCR-methylation-inducing region 2* (*Smi2*) in the *S* locus; the *Smi2* of the dominant *S* locus generates small interfering RNAs (siRNAs), which suppresses the expression of the recessive *S*-locus *SCR* by siRNA-mediated DNA methylation (e.g., *BrS44* > *BrS60* > *BrS40* > *BrS29*, Yasuda *et al.,* 2016). *BoS15* and *BrS60* are interspecific pairs between *B. oleracea* and *B. rapa* based on their high sequence similarity and incompatibility of *B. oleracea BoS15* pollen with *BrS60/BoS18* interspecific hybrid stigmas (Sato *et al.,* 2006). Therefore, *BrS29* could be deduced to be recessive to *BoS15*. The *B. napus* SC line 326 has two *S* haplotypes, *BnS7* (homolog of *BrS29*) in the A subgenome and *BnS6* (homolog of *BoS15*) in the C subgenome, and low expression of *BnSCR7* might confer SC to 326 (Zhai *et al.,* 2014). We speculate that *BnS7* should be recessive to *BnS6*. Then, the *Smi2* was identified in *BnS6* (Figure 1a), which could target promoter of *BnSCR7* (Figure 1b). These results suggest that *BnSCR7* might be suppressed by *BnS6-Smi2*, and then knockout of *BnS6-Smi2* in 326 might recover *BnSCR7* expression and create SI *B. napus*.

To test this hypothesis, three single-guide RNAs (sgRNAs) were designed to target the regions of *BnS6-SMI2* (Figure 1c). Following transformation of these sgRNAs into 326, ten mutants were isolated in T_0 generation, and three independent lines were genotyped in T_1 generation. The deletions or insertions at sgRNA target sites were validated by sequencing (Figure 1c). The three transgene-free homozygous mutants (named SI-326) based on the absence of amplified transgene fragments were used for further analyses (Figure 1d).

The siliques of the three T_1 transgene-free SI-326 lines were first observed. Following self-pollination, their siliques were dramatically shorter than those of 326 (Figure 1e and f), and many siliques were completely empty (33/44 siliques for L3-3, 30/45 for L8-2 and 34/41 for L19-1). The average seed-set of each line was less than one seed per silique, which was less than 326 (24.15 seeds per silique) (Figure 1g). Like 326, SI-326 had pollens with normal viability (Figure 1h). These results indicate that the reduced seed number of SI-326 is not due to reduced pollen viability.

When wild-type 326 stigmas were pollinated with SI-326 pollen (L8-2 or L19-1) in T_2 generation, pollen tube (PT) growth was strongly inhibited (Figure 1i: ii, iii, vi and vii), and the siliques and seed-set were not significantly different from those of SI-326 self-pollination (Figure 1j-l and m-n). By contrast, pollination of SI-326 stigma with 326 pollen resulted in normal PT growth (Figure 1i: i, iv v), and the siliques were normally developed like those of wild-type 326 self-pollination (Figure 1j-l and m-n). These results indicate that self-incompatibility rather than fertility defect causes less self-seed of the SI-326 lines.

Bisulfite sequencing was performed to investigate relation of the transcriptional regulation of *BnSCR7* with DNA methylation in SI-326 and 326, as reported in *B. rapa* (Yasuda *et al.,* 2016). The cytosine methylation levels were not significantly different between 326 and SI-326 in *BnSCR6* promoter regions (Figure 1o and q). By contrast, the cytosine methylation levels of CpG,

© 2021 The Authors. *Plant Biotechnology Journal* published by Society for Experimental Biology and The Association of Applied Biologists and John Wiley & Sons Ltd.
This is an open access article under the terms of the Creative Commons Attribution-NonCommercial License, which permits use, distribution and reproduction in any medium, provided the original work is properly cited and is not used for commercial purposes.

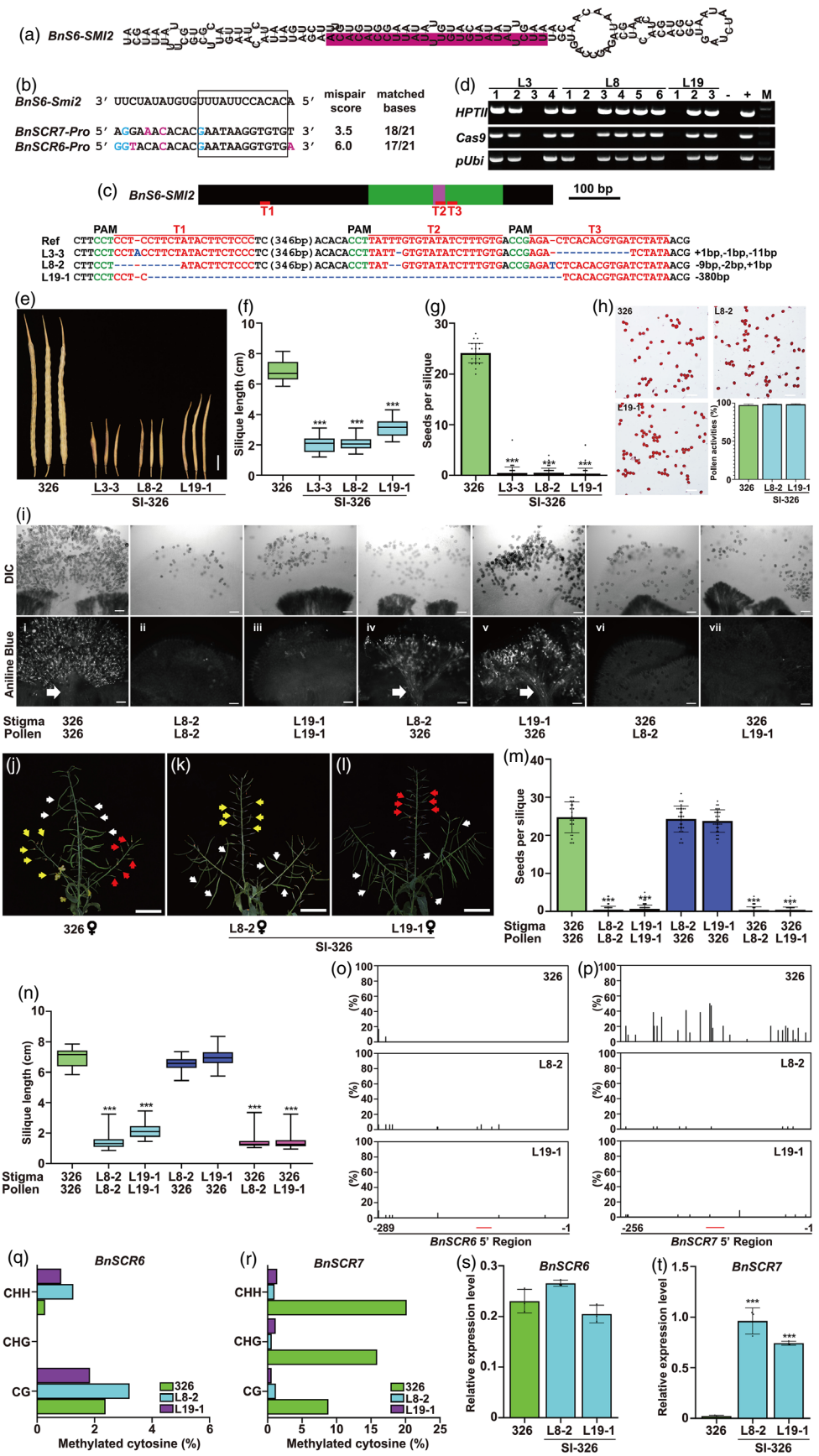
(a) BnS6-SMI2
(b)
BnS6-Smi2 3′ UUCUAUAUGUGUUUAUUCCACACA 5′
mispair score
matched bases
BnSCR7-Pro 5′ AGGAAACACACGAATAAGGTGTGT 3′ 3.5 18/21
BnSCR6-Pro 5′ GGTACACACACGAATAAGGTGTGA 3′ 6.0 17/21
(d)
L3
L8
L19
1 2 3 4 1 2 3 4 5 6 1 2 3 - + M
HPTII
Cas9
pUbi
(c) BnS6-SMI2
T1
T2T3
100 bp
PAM T1 PAM T2 PAM T3
Ref CTTCCTCCT-CCTTCTATACTTCTCCCTC (346bp) ACACACCTTATTTGTGTATATCTTTGTGACCGAGA-CTCACACGTGATCTATAACG
L3-3 CTTCCTCCTACCTTCTATACTTCTCCCTC (346bp) ACACACCTTATT-GTGTATATCTTTGTGACCGAGA----------TCTATAACG +1bp,-1bp,-11bp
L8-2 CTTCCT----------ATACTTCTCCCTC (346bp) ACACACCTTAT--GTGTATATCTTTGTGACCGAGATCTCACACGTGATCTATAACG -9bp,-2bp,+1bp
L19-1 CTTCCTCCT-C----------TCACACGTGATCTATAACG -380bp
(e)
326 L3-3 L8-2 L19-1
SI-326
(f)
Silique length (cm)
326 L3-3 L8-2 L19-1
SI-326
(g)
Seeds per silique
326 L3-3 L8-2 L19-1
SI-326
(h)
326
L8-2
L19-1
Pollen activities (%)
326 L8-2 L19-1
SI-326
(i)
DIC
Aniline Blue
i ii iii iv v vi vii
Stigma 326 L8-2 L19-1 L8-2 L19-1 326 326
Pollen 326 L8-2 L19-1 326 326 L8-2 L19-1
(j)
(k)
(l)
326♀
L8-2♀
L19-1♀
SI-326
(m)
Seeds per silique
Stigma 326 L8-2 L19-1 L8-2 L19-1 326 326
Pollen 326 L8-2 L19-1 326 326 L8-2 L19-1
(n)
Silique length (cm)
Stigma 326 L8-2 L19-1 L8-2 L19-1 326 326
Pollen 326 L8-2 L19-1 326 326 L8-2 L19-1
(o)
326
L8-2
L19-1
-289 -1
BnSCR6 5′ Region
(p)
326
L8-2
L19-1
-256 -1
BnSCR7 5′ Region
(q) BnSCR6
CHH
CHG
CG
326
L8-2
L19-1
Methylated cytosine (%)
(r) BnSCR7
CHH
CHG
CG
326
L8-2
L19-1
Methylated cytosine (%)
(s) BnSCR6
Relative expression level
326 L8-2 L19-1
SI-326
(t) BnSCR7
Relative expression level
326 L8-2 L19-1
SI-326

Figure 1 Generation of self-incompatible *B. napus* by knocking out *BnS6-Smi2* via CRISPR/Cas9. (a) Stem-loop structure of *BnS6-Smi2* precursor. The mature *BnS6-Smi2* is shown in prune. (b) Alignment of *BnSCR6* and *BnSCR7* promoter regions and seed sequence of *BnS6-Smi2*. Mismatched bases and G/U pairs are shown in magenta and blue, respectively. (c) *BnS6-Smi2*, including the sequences outside the siRNA precursor (black boxes), precursor region (green boxes) and mature siRNA (pink box). The red lines under the gene model indicate the sgRNA target sites. The protospacer adjacent motif (PAM) is shown in green. The sgRNA is shown in red. The mutation sites are indicated in blue. (d) Images showing PCR products of *Cas9*, *HPTII* and *pUbi* in SI-326 lines in the T_1 generation. +: pRGEB32 is used as the positive control. -: gDNA of 326 is used as the negative control. (e) The silique phenotypes of 326 and SI-326 at 8 weeks after self-pollination. Scale bars = 1 cm. (f) Quantification of silique length of 326 and SI-326 after self-pollination. (g) Seeds per silique of 326 and SI-326 after self-pollination. (h) Images showing the pollen viability of 326 and SI-326. Quantification of pollen viability of 326 and SI-326 is also shown. Scale bars = 100 μm. (i) Typical DIC (upper panel) and aniline blue staining (lower panel) of 326 and SI-326 pistils after self- or cross-pollination. A bundle of PTs indicates compatible pollination (white arrow). Scale bars = 100 μm. (j)–(l) Images showing the 326 and SI-326 siliques pollinated by 326 and SI-326 pollen. Pollens from 326, L8-2 and L19-1 are indicated by white, yellow and red arrows, respectively. Scale bars = 5 cm. (m) Seeds per silique of 326 and SI-326 after self- or cross-pollination. (n) Quantification of silique length of 326 and SI-326 after self- or cross-pollination. (o) - (p) Percentage of methylation at all cytosine residues in 326 and SI-326 in the promoter regions of *BnSCR6* (nucleotides—289 to −1) (o) and *BnSCR7* (nucleotides −256 to −1) (p). The red line indicates the region homologous to *BnS6-Smi2*. (q)–(r) Percentage of cytosine methylation of CpG, CpNpG and CpNpN in 326 and SI-326 in the promoter regions of *BnSCR6* (nucleotides—289 to −1) (q) and *BnSCR7* (nucleotides—256 to −1) (r). (s)–(t) Expression levels of *BnSCR6* (s) and *BnSCR7* (t) in 326 and SI-326. Data are means ± SD (n = 3) obtained from three biological replicates. *BnActin* is used as the internal control. In (f), (g), (m) and (n), at least three plants per line were sampled for each measurement. Error bars are means ± SD ($n \geq 25$), *** indicate significant differences at $P < 0.001$, based on ANOVA.

CpNpG and CpNpN sequences in *BnSCR7* promoter region in 326 were 8.82%, 15.88% and 20.16%, respectively (Figure 1p and r), which were much higher than those of the *BnSCR6* promoter region (2.38%, 0% and 0.28%). However, the levels of methylated cytosines in this region were significantly lower in both SI-326 lines (Figure 1p and r). Then, there was no difference in *BnSCR6* expression between SI-326 and 326 in unopened floral buds (Figure 1s), whereas the expression of *BnSCR7* was 32-fold higher in SI-326 than in 326 (Figure 1t). These results suggest that *BnS6-Smi2* specifically suppresses *BnSCR7* transcription and that the SI phenotype of SI-326 is caused by decreased DNA methylation in *BnSCR7* promoter region.

To date, very few SI *B. napus* are available for breeding. Here, we generated new SI *B. napus* lines by CRISPR/Cas9 mutation of *BnS6-Smi2*. We demonstrated that *BnS6-Smi2* was essential for maintaining the SC phenotype of 326. Furthermore, we determined that the levels of methylated cytosines in *BnSCR7* promoter were significantly reduced in SI-326, indicating that *BnSCR7* was suppressed by *BnS6-Smi2*-induced DNA methylation. In *B. napus*, the SC accessions that suffer from the same SC reason as accession 326 could possibly be engineered to be SI. The SI lines also could be generated in other Brassicaceae species including *Brassica juncea* and *Brassica carinata*, since the function of siRNA in *S*-locus dominant–recessive interactions is highly conserved (Yasuda *et al.,* 2016). Such transgene-free homozygous mutants containing allele-specific markers could be applied for the breeding of SI *Brassica* plants, thereby accelerating the utilization of heterosis.

Acknowledgements

This research was supported by grants from National Key Research and Development Program of China (2016YFD0101803), and Central Plains Science and Technology Innovation Leading Talents (194200510021).

Conflict of interest

The authors declare no conflicts of interest.

Author contributions

C.D., C.M. and S. D. designed the research. S.D. performed the experiments. J.T., J.S., B.Y., J.W. and T.F. provided laboratory support. C.D., T.Z. and S.D. analyzed the data. C.D., C.M. and S.D. wrote the manuscript. All authors read and approved the manuscript.

References

Chen, K.L., Wang, Y.P., Zhang, R., Zhang, H.W. and Gao, C.X. (2019) CRISPR/Cas genome editing and precision plant breeding in agriculture. *Annu. Rev. Plant Biol.* **70**, 667–697.

Fu, T.D. and Liu, H.L. (1975) Preliminary report on breeding of self-incompatible lines of *Brassica napus*. *Oil Crop China (in Chinese),* **4**, 77–85.

Gao, C.B., Zhou, G.L., Ma, C.Z., Zhai, W., Zhang, T., Liu, Z.Q., Yang, Y. *et al.* (2016) Helitron-like transposons contributed to the mating system transition from out-crossing to self-fertilizing in polyploid *Brassica napus* L. *Sci. Rep.* **6**, 337–355.

Nettancourt, D. (2001) *Incompatibility and Incongruity in Wild and Cultivated Plants*, 2nd ed. Berlin/Heidelberg, New York: Springer-Verlag.

Sato, Y., Sato, K. and Nishio, T. (2006) Interspecific pairs of class II Shaplotypes having different recognition specificities between *Brassica oleracea* and *Brassica rapa*. *Plant Cell Physiol.* **47**, 340–345.

Schopfer, C.R., Nasrallah, M.E. and Nasrallah, J.B.(1999) The male determinant of self-incompatibility in *Brassica*. *Science,* **286**, 1697–1700.

Suzuki, G., Kai, N., Hirose, T., Fukui, K., Nishio, T., Takayama, S., Isogai, A. *et al.* (1999) Genomic organization of the S locus: identification and characterization of genes in *SLG/SRK* region of S_9 haplotype of *Brassica campestris (syn. rapa)*. *Genetics,* **153**, 391–400.

Yasuda, S., Wada, Y., Kakizaki, T., Tarutani, Y., Miura-Uno, E., Murase, K., Fujii, S. *et al.* (2016) A complex dominance hierarchy is controlled by polymorphism of small RNAs and their targets. *Nat. Plants,* **3**, 16206.

Zhai, W., Zhang, J.F., Yang, Y., Ma, C.Z., Liu, Z.Q., Gao, C.B., Zhou, G.L. *et al.* (2014) Gene expression and genetic analysis reveal diverse causes of recessive self-compatibility in *Brassica napus* L. *BMC Genom.* **15**, 1037.

© 2021 The Authors. *Plant Biotechnology Journal* published by Society for Experimental Biology and The Association of Applied Biologists and John Wiley & Sons Ltd.,